

## Carbohydrate Modified Catanionic Vesicles: Probing Multivalent Binding at the Bilayer Interface

Glen B. Thomas,<sup>†</sup> Lenea H. Rader,<sup>†</sup> Juhee Park,<sup>†</sup> Ludmila Abezgauz,<sup>‡</sup> Dganit Danino,<sup>‡</sup> Philip DeShong,<sup>†</sup> and Douglas S. English<sup>\*,§</sup>

*Department of Chemistry and Biochemistry, University of Maryland, College Park, Maryland 20742, Department of Biotechnology and Food Engineering, Technion. Haifa, Israel 32000, and Department of Chemistry, Wichita State University, Wichita, Kansas 67260*

Received September 26, 2008; E-mail: doug.english@wichita.edu

**Abstract:** This article reports on the synthesis, characterization, and binding studies of surface-functionalized, negatively charged catanionic vesicles. These studies demonstrate that the distribution of glycoconjugates in the membrane leaflet can be controlled by small alterations of the chemical structure of the conjugate. The ability to control the glycoconjugate concentration in the membrane provides a method to explore the relationship between ligand separation distance and multivalent lectin binding at the bilayer interface. The binding results using the O-linked glucosyl conjugate were consistent with a simple model in which binding kinetics are governed by the density of noninteracting glucose ligands, whereas the N-linked glycoconjugate exhibited binding kinetics consistent with interacting or clustering conjugates. From the noninteracting ligand model, an effective binding site separation of the sugar sites for concanavalin A of 3.6–4.3 nm was determined and a critical ligand density above which binding kinetics are zeroth order with respect to the amount of glycoconjugate present at the bilayer was observed. We also report cryo-transmission electron microscopy (cryo-TEM) images of conjugated vesicles showing morphological changes (multilayering) upon aggregation of unilamellar vesicles with concanavalin A.

### 1. Introduction

Vesicles have long been of interest to the scientific community as model membrane systems for studying interactions at the bilayer interface. Most studies make use of double-tailed amphiphiles (lipids). However, *single-tailed* amphiphiles can also form vesicles<sup>1–4</sup> and, in particular, simple mixtures of cationic and anionic surfactants, often referred to as catanionic systems, can spontaneously give rise to unilamellar vesicles in water.<sup>4</sup> Catanionic mixtures provide a convenient and an inexpensive route to the formation of ultrastable unilamellar vesicles. A variety of catanionic vesicle-forming systems have been studied with respect to their phase behavior<sup>5–12</sup> but have not been utilized in biophysical studies of molecular interactions at the bilayer interface. Walker and Zasadzinski were the first to functionalize the exterior of catanionic surfactant vesicles by introducing a small amount (0.2 mol %) of a biotinylated

lipid into vesicles formed from cetyltrimethylammonium tosylate (CTAT) and sodium dodecylbenzenesulfonate (SDBS).<sup>13</sup> They then aggregated the vesicles using streptavidin, a tetrameric protein that binds strongly to biotin. Vesicle aggregation was monitored as a function of salt concentration to study the effects of ionic strength and Debye length on intervesicle repulsion. The authors found that aggregation greatly increased when enough salt was added to lower the Debye length to less than the distance of an intervesicular avidin tetramer.

We have decorated the exterior of vesicles with carbohydrate conjugates in a manner similar to the approach used by Walker but using single-tailed glycoconjugates consisting of a glycan portion and an alkyl chain of varying tail length and with different carbohydrate headgroups.<sup>14</sup> Our interest in carbohydrate modification of vesicles stems from the ability to use carbohydrates for cell targeting with high specificity and from the growing interest in glycomics and the need for new tools in this area.<sup>15</sup> Carbohydrates are ubiquitous in organisms and are involved in cell–cell recognition including the infectivity of pathogens, immune response, and reproduction.<sup>16–19</sup> In our initial experiments, we formed SDBS-rich catanionic vesicles

<sup>†</sup> University of Maryland.

<sup>‡</sup> Technion.

<sup>§</sup> Wichita State University.

- (1) Hargreaves, W. R.; Deamer, D. W. *Biochemistry* **1978**, *17*, 3759.
- (2) Gebicki, J. M.; Hicks, M. *Nature* **1973**, *243*, 232.
- (3) Tondre, C.; Caillet, C. *Adv. Coll. Inter. Sci.* **2001**, *93*, 115.
- (4) Khan, A. *Curr. Opin. Colloid Interface Sci.* **1996**, *1*, 614.
- (5) Kondo, Y.; Uchiyama, H.; Yoshino, N.; Nishiyama, K.; Abe, M. *Langmuir* **1995**, *11*, 2380.
- (6) Marques, E. F.; Regev, O.; Khan, A.; Miguel, M. D.; Lindman, B. *J. Phys. Chem. B* **1998**, *102*, 6746.
- (7) Marques, E. F.; Regev, O.; Khan, A.; Miguel, M. D.; Lindman, B. *J. Phys. Chem. B* **1999**, *103*, 8353.
- (8) Herrington, K. L.; Kaler, E. W.; Miller, D. D.; Zasadzinski, J. A.; Chiruvolu, S. *J. Phys. Chem.* **1993**, *97*, 13792.
- (9) Kaler, E. W.; Herrington, K. L.; Murthy, A. K.; Zasadzinski, J. A. *N. J. Phys. Chem.* **1992**, *96*, 6698.

- (10) Berman, A.; Cohen, M.; Regev, O. *Langmuir* **2002**, *18*, 5681.
- (11) Edlund, H.; Sadaghiani, A.; Khan, A. *Langmuir* **1997**, *13*, 4953.
- (12) Yacilla, M. T.; Herrington, K. L.; Brasher, L. L.; Kaler, E. W.; Chiruvolu, S.; Zasadzinski, J. A. *J. Phys. Chem.* **1996**, *100*, 5874.
- (13) Walker, S. A.; Zasadzinski, J. A. *Langmuir* **1997**, *13*, 5076.
- (14) Park, J.; Rader, L. H.; Thomas, G. B.; Danoff, E. J.; English, D. S.; DeShong, P. *Soft Matter* **2008**, *4*, 1916.
- (15) Furukawa, J.-i.; Shinohara, Y.; Kuramoto, H.; Miura, Y.; Shimaoka, H.; Kuroguchi, M.; Nakano, M.; Nishimura, S.-I. *Anal. Chem.* **2008**, *80*, 1094.

and measured the insertion of single-tailed glycolipids with octyl tails into the bilayer. The accessibility of the carbohydrate groups on the vesicle surface was gauged by binding of lectins. Lectins are sugar-binding proteins that interact with their target ligands in a multivalent fashion.<sup>20</sup> Multivalent interactions offer specificity and strength and are prevalent throughout biology.<sup>21</sup> Protein-carbohydrate interactions are facilitated by both the ligand density and spatial arrangements.<sup>20</sup> Our early results showed that surfactant vesicles can be used as scaffolds to present carbohydrates at the necessary density and spatial arrangement for facile and specific binding by lectins.

Lectins have relatively weak affinities with typical  $K_d$  values in the 0.1–1 mM range<sup>20</sup> and therefore rely on multivalent interactions for specificity and strength.<sup>21</sup> Concanavalin A (Con A) is a plant lectin derived from the Jack Bean (*Canavalia ensiformis*) and provides a well-known model system for the study of multivalent lectin binding.<sup>22–27</sup> Con A exists as a tetramer in basic conditions with one saccharide binding site on each monomer and will bind specifically to the carbohydrates  $\alpha$ -D-mannopyranosyl,  $\alpha$ - and  $\beta$ -D-glucopyranosyl, and  $\beta$ -D-fructofuranosyl.<sup>28</sup> Reported values of the saccharide binding site separation distances in tetrameric Con A range from 2.5 to 6.5 nm.<sup>20,28,29</sup> The locations and distances between these binding sites are important because simultaneous involvement of more than one binding site is required for Con A to bind strongly. A single-molecule approach has directly shown that monovalent lectin binding events are transient, whereas bivalent lectin binding events are stronger and have longer lifetimes.<sup>30</sup>

Kiessling and co-workers have made elegant use of synthetic polymeric ligands to acquire quantitative information on the effects of spatial arrangement and density on the binding rates and clustering of Con A.<sup>22,23</sup> They noted a sharp decrease in the binding rate of Con A as a function of ligand density. These studies were performed on synthetic ligands in solution with excellent control over positioning and density. Kiessling and co-workers also found that assembling Con A tetramers using varied molecular scaffolds provided an effective and adjustable method for mediating cell aggregation.<sup>31</sup> Numerous studies have reported on lectin-mediated aggregation of cells<sup>31</sup> and ves-

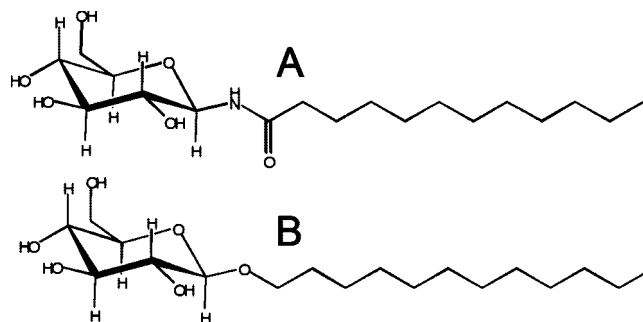


**Figure 1.** Chemical structures of glycoconjugates (A) *n*-dodecanamide- $\beta$ -D-glucopyranoside and (B) *n*-dodecyl- $\beta$ -D-glucopyranoside.

icles<sup>24,25,32–35</sup> for various purposes. In this article, we evaluate Con A-induced multivalent binding using carbohydrate modified cationic vesicles containing different glycoconjugates. Our results point to a promising technique for modeling ligand behavior in an easily characterized biomimetic milieu. We have prepared spontaneously formed surfactant vesicles that incorporate varying amounts of glycoconjugates. These systems provide good models for studies of lectin-induced aggregation to probe selectivity and the effects of carbohydrate length on binding at the membrane interface.<sup>14</sup> Here, we present a method that provides a highly reproducible and simple approach to evaluate the kinetics of lectin-carbohydrate binding in a biomimetic environment in which the membrane surface charge is close to that of most cells,  $\zeta = -50$  mV.

Our method can be performed using vesicles with a wide range of precise carbohydrate surface densities and yields results that are easily described with a tractable model. This novel approach relies on our ability to functionalize the outer membrane leaflet of surfactant vesicles (formed from CTAT and SDBS) in a controlled and systematic fashion. Because of the stable nature of surfactant vesicles, they are ideally suited for this purpose.<sup>36</sup> The vesicles are modified by hydrophobic insertion of the hydrocarbon chain of the glycoconjugates *n*-dodecanamide- $\beta$ -D-glucopyranoside ( $C_{12}NGLu$ , part A of Figure 1) and *n*-dodecyl- $\beta$ -D-glucopyranoside ( $C_{12}OGLu$ , part B of Figure 1). Vesicle preparations are extremely stable against flocculation and can be stored for months.

## 2. Experimental Section

**Materials.** Cetyltrimethylammonium tosylate (CTAT) and *n*-dodecyl- $\beta$ -D-glucopyranoside were obtained from Sigma and sodium dodecylbenzenesulfonate (SDBS) was obtained from TCI America. The protein concanavalin A (Con A) from Jack Bean was obtained from Sigma. Sephadex G-50 Medium was obtained from GE Healthcare. The glycoconjugate *n*-dodecanamide- $\beta$ -D-glucopyranoside was prepared in house. See Supporting Information for details.

**Vesicle Preparation and Characterization.** Vesicles were prepared with the surfactants SDBS, CTAT, and either  $C_{12}OGLu$

- (16) Dwek, R. A. *Chem. Rev.* **1996**, *96*, 683.  
 (17) Larsen, K.; Thygesen, M. B.; Guillaumie, F.; Willats, W. G. T.; Jensen, K. J. *Carbohydr. Res.* **2006**, *341*, 1209.  
 (18) Arnold, J. N.; Wormald, M. R.; Sim, R. B.; Rudd, P. M.; Dwek, R. A. *Annu. Rev. Immunol.* **2007**, *25*, 21.  
 (19) Taylor, M. E.; Drickamer, K. *Introduction to Glycobiology*, 2nd ed.; Oxford University Press: New York, 2006.  
 (20) Wilczewski, M.; Van der Heyden, A.; Renaudet, O.; Dumy, P.; Coche-Guerente, L.; Labbe, P. *Org. Biomol. Chem.* **2008**, *6*, 1114.  
 (21) Mammen, M.; Choi, S. K.; Whitesides, G. M. *Angew. Chem., Int. Ed.* **1998**, *37*, 2755.  
 (22) Cairo, C. W.; Gestwicki, J. E.; Kanai, M.; Kiessling, L. L. *J. Am. Chem. Soc.* **2002**, *124*, 1615.  
 (23) Gestwicki, J. E.; Cairo, C. W.; Strong, L. E.; Oetjen, K. A.; Kiessling, L. L. *J. Am. Chem. Soc.* **2002**, *124*, 14922.  
 (24) Sundler, R. *FEBS Lett.* **1982**, *141*, 11.  
 (25) Luzardo, M. D. C.; Lanio, M. E.; Alvarez, C.; Pazos, I. F.; Figueroa, S.; Verez, V.; Disalvo, E. A. *Colloids Surf., B* **2002**, *26*, 281.  
 (26) Roy, R.; Page, D.; Perez, S. F.; Bencomo, V. V. *Glycoconjugate J.* **1998**, *15*, 251.  
 (27) Bittiger, H.; Shnebli, H. P. *Concanavalin A As a Tool*; Wiley: London, 1976.  
 (28) Becker, J. W.; Reeke, G. N.; Edelman, G. M. *J. Biol. Chem.* **1971**, *246*, 6123.  
 (29) Kanai, M.; Mortell, K. H.; Kiessling, L. L. *J. Am. Chem. Soc.* **1997**, *119*, 9931.  
 (30) Howorka, S.; Nam, J.; Bayley, H.; Kahne, D. *Angew. Chem.* **2004**, *43*, 842.  
 (31) Gestwicki, J. E.; Strong, L. E.; Cairo, C. W.; Boehm, F. J.; Kiessling, L. L. *Chem. Biol.* **2002**, *9*, 163.

- (32) Curatolo, W.; Yau, A. O.; Small, D. M.; Sears, B. *Biochemistry* **1978**, *17*, 5740.  
 (33) Kitano, H.; Sumi, Y.; Tagawa, K. *Bioconjugate Chem.* **2001**, *12*, 56.  
 (34) Guo, C. X.; Boullanger, P.; Liu, T.; Jiang, L. *J. Phys. Chem. B* **2005**, *109*, 18765.  
 (35) Hassane, F. S.; Frisch, B.; Schuber, F. *Bioconjugate Chem.* **2006**, *17*, 849.  
 (36) Kaler, E. W.; Murthy, A. K.; Rodriguez, B. E.; Zasadzinski, J. A. N. *Science* **1989**, *245*, 1371.  
 (37) DuBois, M.; Gilles, K. A.; Hamilton, J. K.; Rebers, P. A.; Smith, F. *Anal. Chem.* **1956**, *28*, 350.

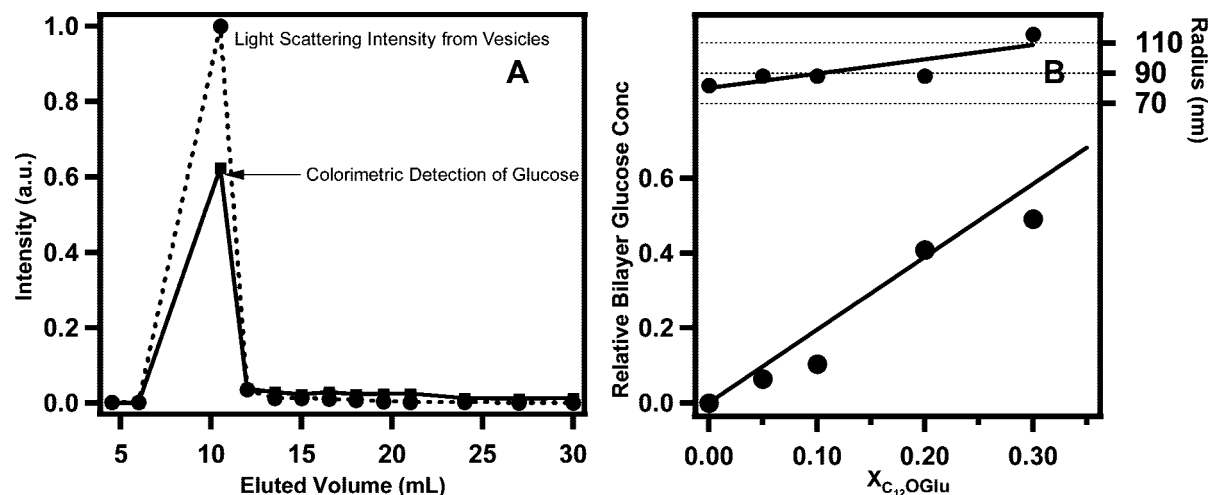


**Figure 2.** Results from SEC analysis of  $C_{12}OGLu$  containing samples. A) Measured values of scattering intensity (circles) and UV–vis intensity for colorimetric detection (squares) as a function of eluted fraction. B) Plot of detected glucose (proportional to UV–vis signal of colorimetric assay) versus initial mole fraction of  $C_{12}OGLu$ .

or  $C_{12}NGLu$ . Millipore water (18 M $\Omega$ ) was added to dry surfactants and then stirred for at least 1 h until no visible surfactant particles remained. Total surfactant concentration was kept constant at  $\sim 27$  mM. The mole ratio of SDBS to CTAT was 3:1 in all cases (70:30 w/w). For vesicle samples containing different mole fractions of  $C_{12}OGLu$  or  $C_{12}NGLu$ , the amount of SDBS and CTAT was adjusted accordingly to keep the stated ratio of ionic surfactants constant. After stirring, the samples were allowed to equilibrate in the dark at room temperature for at least 48 h. Samples were then passed through a 0.45  $\mu m$  syringe filter to remove impurity particles such as dust.

#### Size Exclusion Chromatography and Colorimetric Assay.

After equilibration and filtering, 1 mL of each vesicle sample was run on a  $19.5 \times 3.1$  cm $^2$  size exclusion column packed with Sephadex G-50 Medium. Fractions were collected and saved for analysis by dynamic light scattering (DLS) and by a colorimetric assay<sup>37</sup> used to quantify the amount of  $C_{12}OGLu$  in each fraction collected from SEC. Part A of Figure 2 shows the results of this analysis for a sample containing 0.3 mol fraction of  $C_{12}OGLu$ . For the colorimetric assay, each fraction was diluted 4-fold. To 0.5 mL of the diluted fraction in a test tube was added 0.25 mL of 0.53 M aqueous phenol followed by 1.25 mL of concentrated  $H_2SO_4$ . The test tube was mixed, allowed to cool for 10 m, vortexed, and then allowed to rest at room temperature for 1 h. Ethanol (0.5 mL) was added; after 10 m the absorbance at 490 nm was measured (CHEM2000-UV–vis spectrometer, Ocean Optics, Inc.). When  $C_{12}OGLu$  was present, samples turned yellow-orange in color upon addition of  $H_2SO_4$ . The blank, which contained neat vesicles (lacking  $C_{12}OGLu$ ), phenol,  $H_2SO_4$ , and ethanol in the proportions described above, produced little color in the assay. In Figure 2, it can be seen that all of the glycoconjugate elutes with the vesicle band. In part B of Figure 2, it can be seen that the amount of detected  $C_{12}OGLu$  in the vesicle band increases linearly with the original amount added to the vesicle preparation. This observation and the fact that no glucose was detected in fractions following the vesicle band show that the amount of glucose in the bilayer is quantifiable. Vesicles containing up to 0.3 mol fraction were stable indefinitely and show effectively no change in size relative to neat vesicles. At mole fractions above 0.3, precipitation occurred.

**Aggregation Kinetics Study – Turbidity.** A turbidity assay was used to monitor aggregation kinetics of surface-functionalized vesicles after the addition of Con A. The absorbance at 450 nm

was monitored over time after the addition of buffered Con A to vesicles conjugated with different mole fractions of  $C_{12}OGLu$ . The initial rates were plotted versus the mole fraction of  $C_{12}OGLu$ . A blank containing equal parts vesicle sample and buffer with no Con A was used in each aggregation experiment. Each run was performed by first adding 250  $\mu L$  of vesicle sample to the cuvette, then placing the cuvette in the UV–vis spectrometer, adding 250  $\mu L$  of buffered Con A, then immediately starting acquisition of the kinetics data. The concentration of Con A used was 2.5  $\mu M$ . For each kinetics run, the initial rate was found from the slope of the initial linear region of the absorbance plot. The initial rate of aggregation was monitored to avoid complications associated with a nonlinear response from the formation of large aggregates.<sup>32</sup> To ensure that aggregation was not due merely to adding Con A buffer, control experiments were performed in which 250  $\mu L$  of buffer without Con A was added to vesicles and no significant vesicle aggregation was observed. It can be shown (Figure S.2 in the Supporting Information) that absorbance at 450 nm gives a linear response with respect to vesicle concentration and should therefore give a linear response with an increase in the concentration of small aggregates after the initial addition of Con A. Hence, the initial rate of turbidity increase is linear with respect to small aggregate formation, that is vesicle–Con A–vesicle.

#### Cryogenic Transmission Electron Microscopy (Cryo-TEM).

Cryo-TEM specimens were prepared in a controlled environment vitrification system (CEVS)<sup>38</sup> at controlled temperature of 25  $^{\circ}C$  and 100% relative humidity to avoid evaporation. Samples with Con A were incubated for 30 min prior to their preparation. A drop of each solution was placed on a TEM grid covered with a perforated carbon film and blotted with a filter paper to form a thin solution film on the grid. The samples were then plunged into liquid ethane at its freezing temperature ( $-183$   $^{\circ}C$ ) to form vitrified specimens and stored in liquid nitrogen ( $-196$   $^{\circ}C$ ) until examination. Specimens were examined in a Philips CM120 transmission electron microscope operated at an accelerating voltage of 120 kV using an Oxford CT3500 cryo-specimen holder that maintained the vitrified specimens below  $-175$   $^{\circ}C$ . Specimens were examined in the low-dose imaging mode to minimize electron-beam radiation damage. Images were recorded digitally,<sup>39</sup> on a cooled Gatan MultiScan 791 CCD camera, using the *DigitalMicrograph* software.

(38) Bellare, J. R.; Davis, H. T.; Scriven, L. E.; Talmon, Y. J. *Electron Microsc. Tech.* **1988**, *10*, 87.

(39) Danino, D.; Bernheim-Groswasser, A.; Talmon, Y. *Colloids Surf.*, **A** **2001**, *183*, 113.

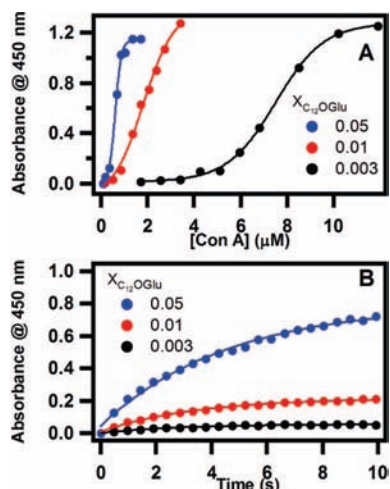
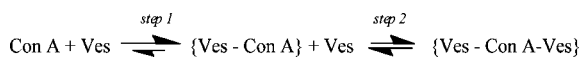


**Figure 3.** Con A-induced agglutination monitored by turbidity. A) Plot illustrating the dependency of Con A-induced agglutination on glucose bilayer concentration. B) As bilayer glucose concentration increases, agglutination rates increase. The experiments in panel B were all carried out with  $[\text{Con A}] = 2.5 \mu\text{M}$ .

**Scheme 1.** Binding Scheme for Con A-Induced Vesicle Aggregation



### 3. Results

Colorimetric assay of SEC fractions for  $\text{C}_{12}\text{Oglu}$  mole fraction samples up to 0.3 indicated that  $\text{C}_{12}\text{Oglu}$  was associated with the same fractions as the vesicles, with effectively no  $\text{C}_{12}\text{Oglu}$  in later fractions. Part A of Figure 2 shows the results from DLS intensity measurements and colorimetric assay on the SEC fractions. Complete association of glycoconjugate with vesicles is indicated by the overlap of DLS intensity and colorimetric assay intensity peaks. Part B of Figure 2 shows the linear relationship between the initial mole fraction of  $\text{C}_{12}\text{Oglu}$  and the amount detected in the vesicle fractions. Hence, the mole fraction of  $\text{C}_{12}\text{Oglu}$  in the vesicle bilayer is identical to the initial mole fraction of  $\text{C}_{12}\text{Oglu}$ .

Simple turbidity studies were conducted to monitor aggregation as a function of the mole fraction of glycoconjugate in the vesicle bilayer. Figure 3 shows results from aggregation studies of three different vesicle preparations that vary in the mole fraction of  $\text{C}_{12}\text{Oglu}$  ( $X_{\text{C}_{12}\text{Oglu}}$ ) present in the bilayer. Part A of Figure 3 shows the measured turbidity of  $\text{C}_{12}\text{Oglu}$  bearing vesicles as a function of Con A concentration. From part A of Figure 3, it can be seen that the Con A concentration required to induce significant aggregation ( $\Delta\text{Abs}(450) > 0.1$ ) increased as  $X_{\text{C}_{12}\text{Oglu}}$  decreased from 0.05 to 0.003. When higher mole fractions were used, above 0.05, the aggregation curves overlaid that of 0.05 in part A of Figure 3. Part B of Figure 3 shows the aggregation kinetics monitored with turbidity for the same samples as part A of Figure 3. For aggregation to occur, the Con A tetramer must bind to two different vesicles, and this requires a two step process in which persistent binding to one vesicle is followed by binding to the second vesicle to form a stable lectin-bridge as shown in Scheme 1.<sup>32</sup>

In these experiments, the Con A concentration is roughly  $10^2$  times greater than the vesicle concentration. Because of the

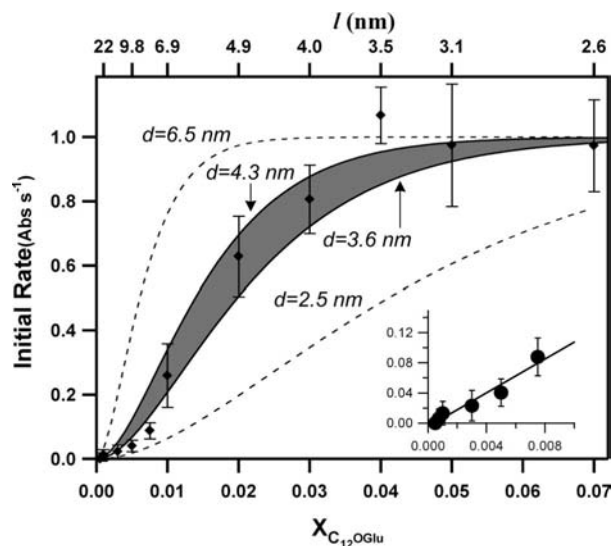


**Figure 4.** Kinetics of vesicle aggregation. Normalized initial rates of vesicle aggregation by Con A are plotted against the bilayer mole fraction of  $\text{C}_{12}\text{Oglu}$ . Experimental data is shown with error bars along with simulated curves using eq 4. Curves were simulated for different  $d = 2.5, 3.6, 4.3,$  and  $6.5 \text{ nm}$ . Inset: Enlargement of linear regime at low concentrations. For all experiments,  $[\text{Con A}] = 2.5 \mu\text{M}$ .

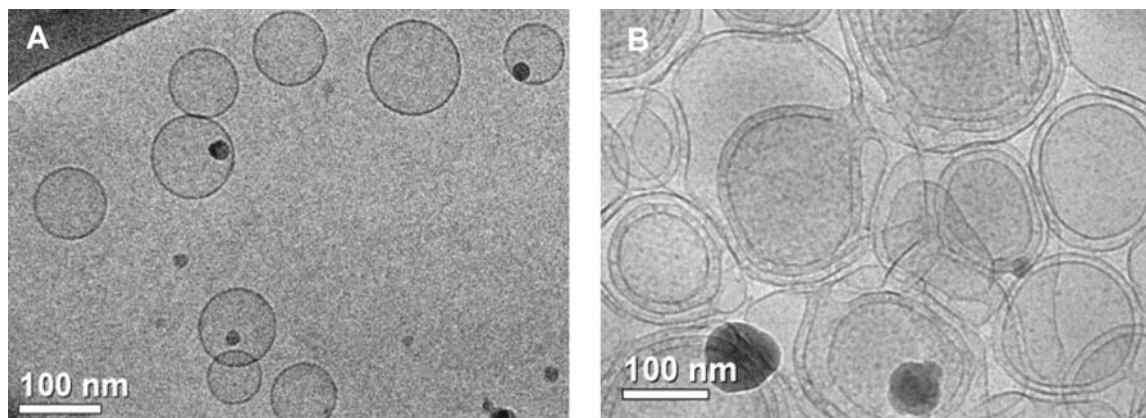
relatively higher concentration of Con A and the great difference between Con A and vesicle diffusion rates, the forward rate for step 2 will be at least 2 orders of magnitude slower than step 1 and therefore rate limiting. Hence, the initial rate of aggregation in Figure 4 is directly proportional to the rate of a vesicle-bound Con A binding at the second vesicle interface. Figure 4 shows the initial rate from turbidity measurements with  $\text{C}_{12}\text{Oglu}$  modified vesicles. In Figure 4, the initial rate of aggregation is plotted over a range of  $X_{\text{C}_{12}\text{Oglu}}$  values, with Con A concentration held constant at  $2.5 \mu\text{M}$ . Figure 5 shows cryo-TEM images of vesicles with  $X_{\text{C}_{12}\text{Oglu}} = 0.005$  before (part A of Figure 5) and after (part B of Figure 5) addition of  $10 \mu\text{M}$  Con A. In part A of Figure 5, unilamellar vesicles exist with diameters of about 100 nm. Upon addition of Con A, the vesicles undergo aggregation and ultimately a morphological change to larger multilamellar vesicles occurs.

Figure 6 compares data gathered from vesicles modified with both  $\text{C}_{12}\text{Oglu}$  and  $\text{C}_{12}\text{Nglu}$ . In Figure 4, at low mole fractions up to 0.01, the rate increased linearly with  $X_{\text{C}_{12}\text{Oglu}}$  and then transitioned to a constant value above  $X_{\text{C}_{12}\text{Oglu}} = 0.03$ . In Figure 6, the rate increased much more rapidly in the case of  $\text{C}_{12}\text{Nglu}$  and the transition occurred at lower mole fraction with saturation at  $X_{\text{C}_{12}\text{Nglu}} = 0.01$ , indicating a significant change in binding kinetics due to the amide functionality that connects the glucose anomeric carbon to the hydrocarbon chain.

### 4. Discussion

Previously, we demonstrated that surface functionalization of SDBS-rich surfactant vesicles with simple glycoconjugates of glucose and lactose resulted in good surface coverage and that the carbohydrate moiety was displayed on the vesicle surface and recognized by the lectins Con A and peanut agglutinin, respectively.<sup>14</sup> Our previous work showed that binding kinetics could be monitored by turbidity and that differences due to surface coverage and carbohydrate length were easily measured. These results suggested that surfactant vesicles would provide an excellent platform for detailed investigation of lectin carbohydrate interactions in a biomimetic

(40) Lahiri, J.; Isaacs, L.; Grzybowski, B.; Carbeck, J. D.; Whitesides, G. M. *Langmuir* **1999**, *15*, 7186.



**Figure 5.** Representative cryo-TEM micrographs of vesicles with  $X_{C_{12}Glu} = 0.005$ . (A) Before mixing with Con A the vesicles are unilamellar and spherical. (B) After mixing with  $10 \mu\text{M}$  Con A the vesicles aggregate and become multilamellar.

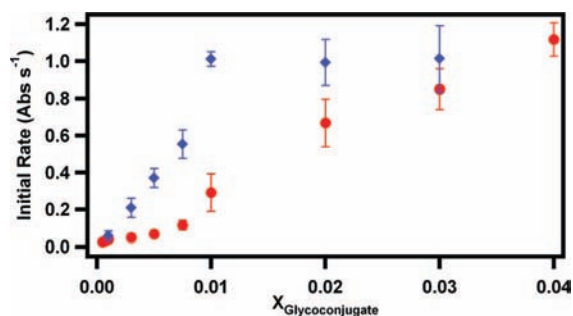


**Figure 6.** Binding kinetics of Con A as a function of bilayer glucose concentration. Vesicles with  $C_{12}NGLu$  are represented by blue diamonds and vesicles with  $C_{12}OGlu$  are represented by red circles.  $[Con A] = 2.5 \mu\text{M}$ .

environment. A significant advantage of surfactant vesicles is that they are simple and cheap to prepare and are stable indefinitely. Hence, development of analysis techniques based on surfactant vesicles is extremely valuable with potential wide appeal. A major goal of the research in this article was to demonstrate the viability of carbohydrate functionalized surfactant vesicles as a useful tool for quantitative investigation into lectin–carbohydrate interactions. The merit of this pursuit is strengthened by the documented need for materials and tools to aid the growing research in glycomics and glycobiology.<sup>15</sup>

Lectin-induced aggregation of vesicles has been used extensively to study protein–carbohydrate interactions but have primarily focused on lipid vesicles.<sup>24,25,32,33</sup> To date, very few studies have utilized surfactant vesicles as platforms for observing protein–ligand interactions.<sup>13,14</sup> Surfactant vesicles are more stable than most lipid preparations and they can be stored for long periods prior to use. For instance, the vesicles shown in part A of Figure 5 were approximately 6 weeks old. The size distribution is similar to that obtained for the freshly prepared sample by DLS. In separate experiments, we have stored  $C_{12}OGlu$  containing vesicles for up to two months with no measurable degradation as determined by DLS and aggregation studies. The same changes in turbidity are noted when a fresh or aged sample is mixed with Con A. A cryo-TEM micrograph of the aggregated sample from part A of Figure 5 is shown in part B of Figure 5. This figure displays an interesting and unexpected result: Con A-induced aggregation of surfactant vesicles caused a morphological change from small unilamellar vesicles to large multilamellar vesicles with several layers. Further study is necessary to determine the driving force of this

process. A possible explanation is that binding with Con A brought vesicles close together such that smaller vesicles were engulfed by larger vesicles. Bilayer fluidity would allow rearrangement into stacked membranes held together by Con A molecules located between the bilayers. The cryo-TEM images show clearly that aggregation is responsible for the turbidity changes documented by Figures 3 and 4. The robust long-term stability of surfactant vesicles, the ease with which they can be controllably functionalized, and the low cost of CTAT and SDBS make this system highly valuable as a new platform for evaluating lectin–carbohydrate interactions. Below, we discuss how our results with these novel materials can be used to quantify the effective separation distance of carbohydrate binding sites in Con A and also detect ligand clustering.

The relative positions and separation distances of sugar binding sites in multimeric lectins is critical for gaining a molecular-level understanding of the multivalent interactions involved in protein recognition of glycans. Such knowledge can be useful for designing polyvalent ligands for research or as lectin inhibitors. The trend observed in Figure 4 indicates a transition between two kinetic regimes associated with an increase in  $C_{12}OGlu$ . At very low  $C_{12}OGlu$  concentration,  $X_{C_{12}OGlu} < 0.01$ , the initial rate of aggregation increases linearly; see the inset of Figure 4. This indicates that the formation of stable lectin-bridges, as indicated in Scheme 1, is a function of the surface density of  $C_{12}OGlu$ . Above  $X_{C_{12}OGlu} = 0.01$ , the rate increases sharply and plateaus around 0.04, indicating a transition from first-order to zeroth-order dependence on  $C_{12}OGlu$ . This transition suggests that a critical surface density is reached at which Con A binding attains a maximum velocity. Similar behavior has been observed with carbohydrate modified lipid vesicles.<sup>32,33</sup> We have devised a simple model to describe the trend observed in Figure 4. The initial binding rate will depend directly on the frequency of collisions ( $\nu_{coll}$ ) between a vesicle–Con A complex (i.e., Ves–Con A in Scheme 1) and a second vesicle surface. This frequency scaled by a probability factor ( $\phi$ ) to account for orientation, kinetic energy, and ligand density is proportional to the initial rate of aggregation:

$$\text{rate} \propto \nu_{coll} \phi \quad (1)$$

In our experiments, Con A and vesicle concentrations are held constant and therefore  $\nu_{coll}$  does not change. Hence, the variation in initial rate observed in Figure 4 must be due to  $\phi$ . This variation can be captured by a simple model based on multivalent interactions that assumes: i) noninteracting randomly

distributed ligands on the membrane surface, ii) an effective sampling area,  $A_{\text{sample}}$ , is contacted by the Con A tetramer during a collision with the membrane surface, and iii) the presence of two ligands in  $A_{\text{sample}}$  is required for persistent binding and aggregation. The first criterion invokes a Poisson distribution to describe the ligand spatial distribution at the membrane interface. For the second requirement, the average effective separation between binding sites in Con A defines  $A_{\text{sample}}$ ; a similar approach has been used to describe the binding of the enzyme carbonic anhydrase to target substrates of varying ligand density.<sup>40</sup> The third requirement is supported by the fact that Con A has a significantly lower  $K_d$  value for multivalent ligands relative to monovalent ligands.<sup>41–43</sup> To induce aggregation, the Con A tetramer must bind two glycosyl residues for a protein-vesicle collision to result in persistent binding. Using an average headgroup area of  $0.48 \text{ nm}^2$  per molecule,<sup>13</sup> we obtained the average number of glucose residues per square nanometer ( $\rho$ ) as:

$$\rho = \frac{X_{\text{C}_{12}\text{OGlu}}}{0.48 \text{ nm}^2} \quad (2)$$

We can use this value of  $\rho$  to determine the probability of a Con A tetramer encountering at least two residues in a single collision. Our model assumes that when a vesicle-bound Con A tetramer collides at the interface of a second vesicle, it sweeps out an effective target area ( $A_{\text{sample}} = \pi d^2$ ) on the bilayer surface determined by the effective binding site separation distance of the tetramer  $d$ . The average number of ligands encountered per collision ( $\mu$ ) will then be:

$$\mu = \rho A \quad (3)$$

Now it is possible to calculate the probability that a Con A tetramer colliding with the exterior bilayer will encounter two or more glycosyl residues based on a Poisson distribution of glycosyl sites:

$$P(N \geq 2) = \sum_{N=2}^{\infty} \frac{\mu^N}{N!} e^{-\mu} \quad (4)$$

Eq 4 gives the probability that the number of glycoconjugates within  $A_{\text{sample}}$  will be  $N \geq 2$ . In Figure 4, we show a range of simulated curves generated using eqs 1–4 with different assumed values of  $d$ . Our model reproduces the observed kinetic trend. The two extreme curves are for the limits of the literature values for  $d$ .<sup>20,28,44</sup> The shaded central region is the range of  $3.6 < d < 4.3 \text{ nm}$ . The best fit based on a chi-squared analysis is given by the curve corresponding to  $3.9 \text{ nm}$ . Our data suggests an effective binding site separation distance of  $3.9 \text{ nm}$  for Con A, well within the range of  $2.5\text{--}6.5 \text{ nm}$  found in various literature sources.<sup>20,28,44</sup>

The top axis of Figure 4 gives the calculated average separation between glucose residues ( $l$ ) over the range of  $X_{\text{C}_{12}\text{OGlu}}$  where  $l = ((0.48)/(X_{\text{C}_{12}\text{OGlu}}))^{1/2} \text{ nm}$ . When  $X_{\text{C}_{12}\text{OGlu}} < 0.005$ ,

glycoconjugate spacing exceeds the Con A binding site separation distance and binding kinetics are pseudofirst order with respect to  $\text{C}_{12}\text{OGlu}$ . At these low  $X_{\text{C}_{12}\text{OGlu}}$  values, experimental deviation of forward reaction rates from the model is likely due to the competing backward reaction. At  $X_{\text{C}_{12}\text{OGlu}} > 0.01$  the initial rate increases rapidly finally converting to zeroth order at  $l \approx 3.5 \text{ nm}$ . This transition is complete when  $l < d$  and the ligand density is approximately  $0.083 \text{ residues/nm}^2$ . At this density of glycoconjugate, the Con A always encounters two or more glucose ligands during a vesicle collision. Saturation kinetics of this sort has been observed in other lectin-induced aggregation studies.<sup>32,33</sup> Our current model assumes no clustering of ligands, and the good fit to the data suggests that ligand clustering does not play a role here. Studies using cyclodextrin vesicles have shown multivalent host-guest interactions can cause clustering.<sup>45</sup> However, receptor-induced ligand clustering is unlikely to effect initial rate measurements given the short duration of the measurement but would certainly affect equilibrium.

In an effort to help test our model, we have synthesized an N-linked analog of  $\text{C}_{12}\text{OGlu}$ . On the basis of our previous experience with glycoconjugates attached to gold surfaces, there is strong evidence to indicate that O-linked and N-linked glycoconjugates will interact differently in a fluid bilayer.<sup>46</sup> On gold surfaces, Fourier transform infrared spectroscopy suggested that high packing densities were facilitated by hydrogen bonding between amide groups on adjacent immobilized molecules. In a fluid bilayer, it is anticipated that hydrogen bonding could cause ligand clustering of the N-linked glycoconjugate,  $\text{C}_{12}\text{NGlu}$ . Such clustering should result in a measurable deviation from the behavior observed for  $\text{C}_{12}\text{OGlu}$ . Because these clusters would spontaneously self-assemble, it was anticipated that binding and aggregation would be facilitated in the N-linked system. Figure 6 shows a comparison of the initial rates for both glycoconjugates. As anticipated, aggregation kinetics was much more accelerated at low concentrations for  $\text{C}_{12}\text{NGlu}$  relative to  $\text{C}_{12}\text{OGlu}$ . This observation is consistent with the formation of glycoconjugate-rich domains that enhance multivalent interactions, similar to the formation of lipid rafts observed in lipid bilayers. Other stabilizing interactions favoring ligand clustering include hydrophobic interactions of the surfactant tails and hydrophobic interactions between faces of glucose residues. The latter interaction would likely not be present with other saccharide residues (e.g., mannose or galactose) due to differing position of hydrophilic hydroxyl residues in the saccharide structure. Ligand clustering would cause Con A to encounter two or more glucose residues in its effective sampling area at lower  $\text{C}_{12}\text{NGlu}$  concentrations. This would account for the rapid binding rate increase as a function of ligand concentration as well as the saturation of kinetics at lower ligand concentrations compared to  $\text{C}_{12}\text{OGlu}$ -conjugated vesicles. The innate stability and ease of preparation of carbohydrate-modified catanionic surfactant vesicles offers a powerful new technique for probing multivalent lectin-carbohydrate interactions.

## 5. Conclusions

In summary, we demonstrated the use of carbohydrate functionalized, spontaneously formed surfactant vesicles as a model platform for investigating protein-carbohydrate interac-

(41) Dimick, S. M.; Powell, S. C.; McMahon, S. A.; Moothoo, D. N.; Naismith, J. H.; Toone, E. J. *J. Am. Chem. Soc.* **1999**, *121*, 10286.

(42) Ebara, Y.; Okahata, Y. *J. Am. Chem. Soc.* **1994**, *116*, 11209.

(43) Dam, T. K.; Roy, R.; Das, S. K.; Oscarson, S.; Brewer, C. F. *J. Biol. Chem.* **2000**, *275*, 14223.

(44) Bakowsky, U.; Rettig, W.; Bendas, G.; Vogel, J.; Bakowsky, H.; Harnagea, C.; Rothe, U. *Phys. Chem. Chem. Phys.* **2000**, *2*, 4609.

(45) Lim, C. W.; Ravoo, B. J.; Reinhoudt, D. N. *Chem. Commun.* **2005**, 5627.

(46) Kadalbajoo, M.; Park, J.; Opdahl, A.; Suda, H.; Kitchens, C. A.; Garno, J. C.; Batteas, J. D.; Tarlov, M. J.; DeShong, P. *Langmuir* **2007**, *23*, 700.

tions. The surfactant vesicle system consists of negatively charged, unilamellar vesicles that can be stored for months with no measurable degradation. Glycoconjugate compositions up to 0.3 mol fraction have been prepared and show excellent colloidal stability. Aggregation studies were used to measure Con A binding rates from which a simple model was employed to estimate the effective binding site separation of the Con A tetramer. We found good agreement between the literature values of Con A binding site separation distance and values obtained from a Poisson analysis of the O-linked glucoconjugate. However, the binding of Con A to the N-linked glycoconjugate indicated that C<sub>12</sub>NGlu forms hydrogen bonded clusters in the membrane. Finally, we have observed that a morphological change from small unilamellar vesicles to larger multilamellar vesicles occurs upon Con A-induced aggregation of small glycoconjugate-functionalized unilamellar vesicles. Further stud-

ies will determine the feasibility of isolating large multilamellar vesicles in solution for diverse applications.

**Acknowledgment.** This work was supported in part by the U.S. National Science Foundation under award CTS-0608906. D.S.E. acknowledges financial support from the Maryland Technology Development Corporation, Wichita State University and from SD Nanosciences. D. Danino thanks the Russell Berrie Nanotechnology Institute (RBNI) for partial support of this project.

**Supporting Information Available:** Procedures for synthesis of several compounds, size exclusion chromatography, dynamic light scattering, and concanavalin A turbidity assay. This material is available free of charge via the Internet at <http://pubs.acs.org>.

JA8076439